Mechanistic determinants of effector-independent motor memory encoding

Adarsh Kumar[a,b], Gaurav Panthi[b,c], Rechu Divakar[b], and Pratik K. Mutha[b,c,1]

[a]Department of Mechanical Engineering, Indian Institute of Technology Gandhinagar, Gujarat 382355, India; [b]Center for Cognitive and Brain Sciences, Indian Institute of Technology Gandhinagar, Gujarat 382355, India; and [c]Department of Biological Engineering, Indian Institute of Technology Gandhinagar, Gujarat 382355, India

Edited by Peter L. Strick, University of Pittsburgh, Pittsburgh, PA, and approved June 8, 2020 (received for review January 20, 2020)

Coordinated, purposeful movements learned with one effector generalize to another effector, a finding that has important implications for tool use, sports, performing arts, and rehabilitation. This occurs because the motor memory acquired through learning comprises representations that are effector-independent. Despite knowing this for decades, the neural mechanisms and substrates that are causally associated with the encoding of effector-independent motor memories remain poorly understood. Here we exploit intereffector generalization, the behavioral signature of effector-independent representations, to address this crucial gap. We first show in healthy human participants that postlearning generalization across effectors is principally predicted by the level of an implicit mechanism that evolves gradually during learning to produce a temporally stable memory. We then demonstrate that interfering with left but not right posterior parietal cortex (PPC) using high-definition cathodal transcranial direct current stimulation impedes learning mediated by this mechanism, thus potentially preventing the encoding of effector-independent memory components. We confirm this in our final experiment in which we show that disrupting left PPC but not primary motor cortex after learning has been allowed to occur blocks intereffector generalization. Collectively, our results reveal the key mechanism that encodes an effector-independent memory trace and uncover a central role for the PPC in its representation. The encoding of such motor memory components outside primary sensorimotor regions likely underlies a parsimonious neural organization that enables more efficient movement planning in the brain, independent of the effector used to act.

movement | learning | generalization | posterior parietal cortex

Skilled motor behavior, from a graceful ballet move to a tennis ace, is crucially dependent on the ability to learn new movement patterns and adapt existing ones to novel environments. Motor learning results in the formation of a motor memory that enables more efficient movement planning, better movement corrections, and more robust predictions about the outcomes of our actions. Theories have long suggested that multiple mechanisms operating at different timescales drive motor learning in humans. These range from cognitive or strategic processes that afford rapid behavioral gains to more implicit mechanisms that lead to slower, gradual changes in performance (1, 2). Newer work, especially in error-driven motor adaptation, in which the motor memory comprises internal neural representations of the physics of the body and the environment, has also provided elegant mathematical bases for these ideas (3–5).

Deeper insight into the mechanisms that drive learning and characteristics of the motor memory can be obtained by examining how learning generalizes to untrained conditions, a principle that applies to other memory systems as well (6, 7). In humans, there is longstanding evidence that learning movements with one effector generalizes to other effectors (8–13). This occurs because the acquired memory includes components that are effector-independent. Despite the clear phenomenological demonstration of intereffector generalization over many studies, and an appreciation that it can be functionally exploited, for example in neurorehabilitation, a principled understanding of the mechanisms that encode the effector-independent representation, and its neuroanatomical basis, has been lacking.

One theory in motor adaptation is that effector-independent memory components are acquired via the early, fast-acting, strategic mechanisms that bring about rapid changes in motor behavior (10, 14). The idea is that, since a generic strategy, or a broad "algorithm" to counter errors, is learned, it is available to the untrained limb. However, this view can be challenged based on other results (15, 16), rendering the mechanistic determinants of these representations unresolved. A compelling alternative is that such representations are encoded by slower, implicit mechanisms that evolve gradually during learning. Since these mechanisms bring about more robust, temporally stable updates to internal representations of the relationship between arm motion and its sensory consequences, and also enable long-term retention (17), it may be more optimal to make these available to an untrained effector. A critical prediction of this hypothesis is that generalization across effectors, the signature of the effector-independent representation, should be strongly predicted by the state of the slow rather than the fast process when both combine to drive learning. In our first experiment, we systematically manipulate the number of learning trials to capture different levels of these processes and demonstrate that this is indeed the case.

Significance

Humans are sensitive to errors in their movements and learn from them. Years of work in sensorimotor neuroscience has shown that learning actions with one effector engenders motor memories that comprise effector-independent representations. We probe the mechanisms and neuroanatomical substrates that are causally associated with the encoding of these memory components. Using a combination of behavioral experiments, computational modeling, and brain stimulation in humans, we show that such representations are encoded via a parietal-dependent, implicit mechanism that evolves gradually during learning. By uncovering the computations underlying encoding of effector-independent memories and assigning a causal role to posterior parietal cortex, our results compel an appreciation of the contributions of association cortices to the learning and memory of new motor acts.

Author contributions: A.K., G.P., R.D., and P.K.M. designed research; A.K., G.P., and R.D. performed research; A.K., G.P., R.D., and P.K.M. analyzed data; and A.K., G.P., and P.K.M. wrote the paper.

The authors declare no competing interest.

This article is a PNAS Direct Submission.

Data deposition: Data supporting the findings of the study are available on Figshare at https://figshare.com/articles/Kumar_et_al_2020_data/12416426.

[1]To whom correspondence may be addressed. Email: pm@iitgn.ac.in.

This article contains supporting information online at https://www.pnas.org/lookup/suppl/doi:10.1073/pnas.2001179117/-/DCSupplemental.

First published July 9, 2020.

Neuroanatomically, learning-related plasticity is known to be widespread in the brain (18). Yet, a memory built via error-based learning of new dynamics and visuomotor relationships is believed to be encoded chiefly in primary motor cortex or M1 (19, 20). Paradoxically, modulation of M1 activity fails to influence the effector-independent component (21), suggesting that the neural locus for such representations may lie outside this region. We consider the alternative possibility that the posterior parietal cortex (PPC) is causally engaged in the encoding and representation of such memory components. Some functional neuroimaging work has revealed overlapping areas of activation within the intraparietal sulcus when different effectors are moved in a similar manner (22, 23), implying the existence of function-based representations that are not specifically tied to a particular effector in these areas. This appears to hold even at the neuronal level, and is not limited to only the level of the entire region (24). Yet, these findings have been countered with electrophysiological (25, 26) and imaging (27) results that suggest that PPC representations are effector-specific. Thus, based on the strength of the current evidence, it is difficult to be certain whether effector-independent representations are encoded in areas that include the PPC. Besides, the imaging studies do not specify the mechanisms that encode such representations, and are also somewhat limited in terms of establishing causality of the association.

A persuasive, alternate way to test the causal role of PPC in encoding effector-independent memory components in humans may be to exploit intereffector generalization and probe if 1) disrupting PPC prior to learning impedes the slowly evolving learning process (since, as our first experiment reveals, it is this process that predicts generalization) and 2) disrupting PPC activity postlearning blocks generalization. We pursue this line of thought and demonstrate that high-definition cathodal transcranial direct current stimulation (hd-tdcs) delivered near the left intraparietal sulcus produces these effects. Taken together, our findings provide evidence for a critical role of the PPC in encoding effector-independent representations of a motor memory via gradually evolving, implicit learning mechanisms.

Results

In experiment 1 (Fig. 1*A*), healthy human participants made point-to-point reaches with their left or right arm under conditions in which the visually seen motion of the hand (represented by a screen cursor) was rotated by 30° relative to actual hand motion. People typically learn to modify their movement direction by anticipating the effects of the rotation, and this learning is achieved through the operation of more than one learning mechanism. Critically, we varied the number of learning trials (40, 80, 160, 320) across different participant groups in order to systematically control the levels of these constituent learning processes.

Naïve Learning Was Not Different between Arms or Learning Trial Sets. Fig. 1*B* (solid lines) shows the movement (cursor) trajectories of representative subjects in various groups upon initial exposure to the rotation. As is evident, the trajectories were similarly perturbed across all these participants. Direction errors during early learning were not different between arms or learning trials experienced (arm, $F_{1,56} = 0.9861$, $P = 0.3250$, $\eta^2_p = 0.017$; trial set, $F_{3,56} = 1.2874$; $P = 0.2877$, $\eta^2_p = 0.064$; interaction, $F_{3,56} = 0.8276$; $P = 0.4843$, $\eta^2_p = 0.042$). Learning progressed via a reduction in errors, with trajectories becoming straighter (Fig. 1*B*, dotted lines) and mean direction error reducing over trials (Fig. 1*C*). Performance at the end of learning also did not differ between the experimental conditions (arm, $F_{1,56} = 0.0778$, $P = 0.7813$, $\eta^2_p = 0.001$; trial set, $F_{3,56} = 0.0096$, $P = 0.9987$, $\eta^2_p = 0.0005$; interaction, $F_{3,56} = 0.2508$, $P = 0.8605$, $\eta^2_p = 0.013$). Thus, naïve learning occurred in a fairly canonical manner across the different groups.

Generalization Was Asymmetric and Scaled with Number of Learning Trials. Postlearning generalization across effectors, the manifestation of the effector-independent representation encoded via learning, was then probed by exposing the opposite, untrained arm to the same perturbation for 40 trials. Generalization was assayed by comparing direction errors on these trials to those on naïve learning trials of the same arm. Consistent with past work (10, 13), there was no generalization from the right arm to the left. Movement trajectories of the left arm on generalization trials overlapped with those of its naïve learning trials (Fig. 2*A*), indicating that prior right arm learning provided no benefit to the left arm. Average direction errors were not different between the learning and generalization blocks across learning trial sets, confirming that generalization did not occur (block, $F_{1,56} = 0.0196$, $P = 0.8890$, $\eta^2_p = 0.0003$; trial set, $F_{3,56} = 0.6076$, $P = 0.6128$, $\eta^2_p = 0.031$; interaction, $F_{3,56} = 1.5716$, $P = 0.2064$, $\eta^2_p = 0.077$; Fig. 2*A*, bar plots, and *SI Appendix*, Fig. S1*A*).

In contrast, learning generalized quite well from the left arm to the right. Remarkably, we found that the extent of generalization

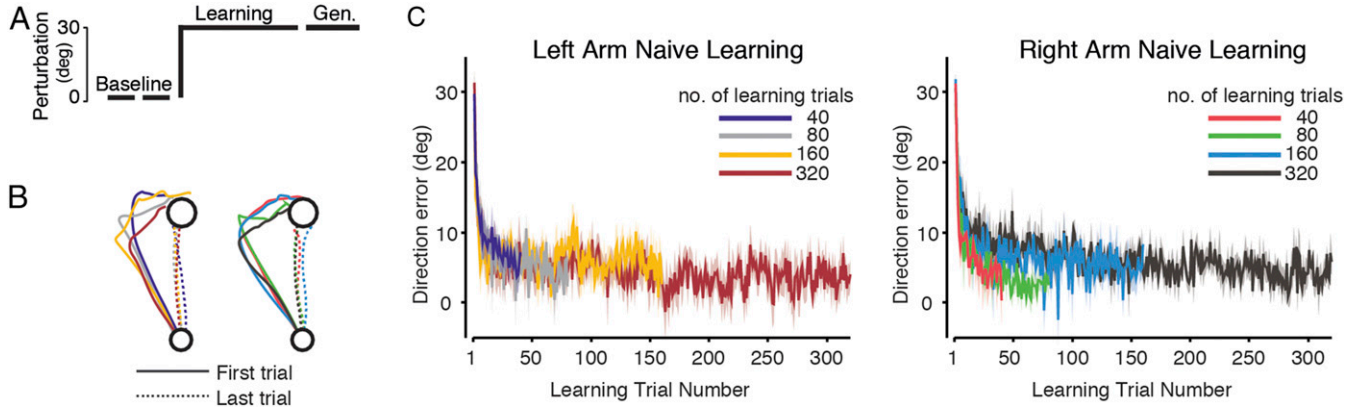

Fig. 1. Naïve learning. (*A*) Participants ($n = 64$) performed baseline (no perturbation) trials with their left and right arms, followed by a block where they learned, over varying numbers of trials, to adapt their movements to a 30° visuomotor rotation with one of the arms ($n = 32$ each). Generalization was then tested by exposing the opposite, untrained arm to the same rotation. (*B*) Movement (cursor) trajectories on the first (solid lines) and last (dotted lines) learning trials. The different colors represent the number of learning trials experienced. Trajectories were curved initially, but became straighter with learning. Data are for representative participants. (*C*) Group-averaged ($n = 8$ per group) direction errors plotted across learning trials. Shaded regions are SEM. Errors reduced similarly across arms and learning trial sets.

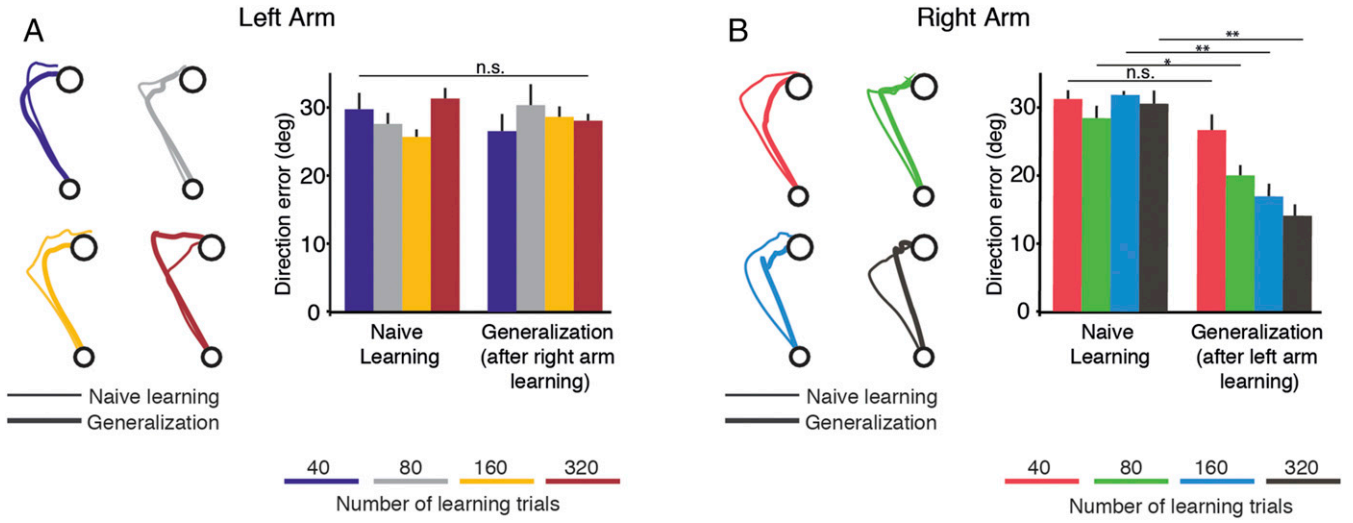

Fig. 2. Generalization. (*A* and *B*, *Left*) Movement (cursor) trajectories on learning (thin lines) and generalization (thick lines) trials. Trajectories on learning and generalization trials overlapped substantially for the left arm. This was not the case for the right arm, where trajectories were directed closer to the target on generalization trials. (*Right*) Bar plots show group-averaged ($n = 8$ per group) direction errors ± SEM on initial learning and generalization trials. There was no difference for the left arm, but, for the right arm, errors on generalization trials became increasingly smaller as the number of learning trials increased. ns, not significant (*$P = 0.0129$; **$P < 0.0001$).

was sensitive to the number of prior learning trials experienced. There was a clear separation of right arm trajectories on the learning and generalization trials, with the cursor being directed increasingly closer to the target on generalization trials as the number of prior learning trials increased (Fig. 2*B*). This was reflected as smaller direction errors on generalization trials compared to naïve (Fig. 2*B*, bar plots, and *SI Appendix*, Fig. S1*B*), a pattern that was upheld in subsequent statistical tests (significant interaction between block and learning trial set, $F_{3,56} = 5.9127$, $P = 0.0014$, $\eta^2_p = 0.24$; post hoc tests, 40 trial set, $P = 0.5139$; 80 trials, $P = 0.0129$; 160 trials, $P < 0.0001$; 320 trials, $P < 0.0001$). A direct comparison of errors on generalization trials showed differences across learning trial sets ($F_{3,28} = 9.7971$, $P = 0.0001$, $\eta^2_p = 0.51$). A one-sided Dunnett's test showed that the 320-trial group had significantly lower errors compared to the 40-trial ($P < 0.0001$) and 80-trial ($P = 0.0283$) groups but not the 160-trial group ($P = 0.2657$). Although not a direct measure of generalization magnitude itself, the saturating trend in the errors suggested that generalization to the right arm increased as more trials were experienced with the left arm, but leveled off with more extended practice.

Generalization Was Predicted by the State of a Gradual Learning Mechanism. To examine the relationship between the mechanisms that drive learning and intereffector generalization, we considered a multiprocess learning framework (3) and asked whether the observed generalization could be predicted by the level of the slow, implicit (but not the fast) learning process in this model (Fig. 3*A*). We found that the group-averaged generalization magnitude tracked neither the total learning (Fig. 3 *B*, *Left*) nor the fast process (Fig. 3 *B*, *Middle*), but closely tracked the growth of the slow process (Fig. 3 *B*, *Right*). There was a remarkably strong association between the model-predicted level of this gradually evolving mechanism and the experimentally observed generalization amplitude (Fig. 3 *C*, *Right*). In contrast, there was no consistent pattern in terms of generalization that could be predicted from the state of the fast process (Fig. 3 *C*, *Middle*) or the total learning (Fig. 3 *C*, *Left*). Critically, the relationship between generalization and the slow state was just as robust when generalization was computed on a within-participant basis (*SI Appendix*, Fig. S2), and also when the fast and slow states were simulated from model fits to data from an additional "control" experiment with a completely different perturbation protocol (*SI Appendix*, Fig. S3). A multiple linear regression of the form [generalization = β_1 * $x_s(n)$ + β_2 * $x_f(n)$], where $x_s(n)$ and $x_f(n)$ represent values of the slow and fast processes at the end of the n^{th} learning trial, fit the generalization data very well ($r^2 = 0.9925$, $F_{2,2} = 132.4$, $P = 0.007$). We also found a significant contribution of the slow process (95% CI for $\beta_1 = 0.974 \pm 0.42$), but not the fast process (95% CI for $\beta_2 = -0.021 \pm 0.38$). In sum, generalization, a reflection of an effector-independent motor memory component, was best predicted by the level of a gradually evolving learning mechanism.

PPC Disruption Impeded Learning Based on the Slow Process. Next, we probed whether disrupting parietal processing affected memory encoding by impeding the slow process. In our second experiment (Fig. 4*A*), we delivered cathodal hd-tdcs over left or right PPC, near the intraparietal sulcus (Fig. 4*B*). Cathodal stimulation decreases the probability of spontaneous neuronal activation and temporarily "inhibits" the activity of the region over which it is applied (28). We observed that initial exposure to the rotation produced effects that were not different between participants who received real or sham stimulation (trajectories shown in solid lines in Fig. 4 *C* and *D*); this was also confirmed statistically ($F_{3,60} = 0.3895$, $P = 0.7610$, $\eta^2_p = 0.019$). Notably, learning progressed differently for the group that received left PPC stimulation relative to others. While movements of participants in other groups were directed relatively straight toward the target during the late learning stage, trajectories of those who received left PPC stimulation continued to be curved (compare dotted trajectories in Fig. 4 *C* and *D*; also see *SI Appendix*, Fig. S4). At the end of learning, this group continued to show larger direction errors ($F_{3,60} = 7.8326$, $P = 0.0002$, $\eta^2_p = 0.281$; Fig. 4 *C* and *D*) than sham ($P = 0.0003$) as well as the right PPC stimulation groups ($P = 0.0126$).

Comparison of parameters of the multirate model fit to this learning data indicated that left PPC hd-tdcs only impaired the slow process. We found a significant group difference for the slow learning rate B_s ($H_3 = 8.436$, $P = 0.037$) but not other parameters (A_s, $H_3 = 3.152$, $P = 0.368$; A_f, $H_3 = 0.971$, $P = 0.808$; B_f, $H_3 = 2.451$, $P = 0.484$). Post hoc comparisons confirmed that B_s was significantly lower for the left PPC stimulation group

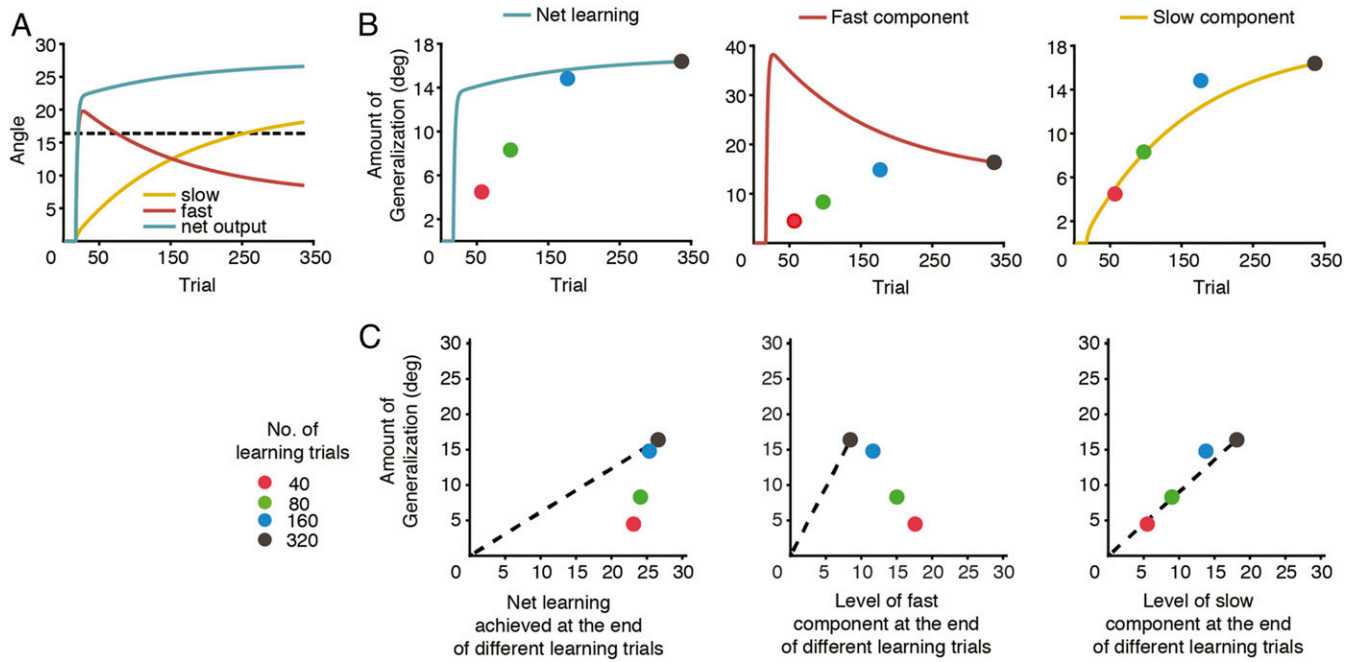

Fig. 3. Generalization was best associated with the slowly evolving process of a multirate learning model. (*A*) The multirate model has "fast" (maroon) and "slow" (orange) processes that are summed to yield the net output (blue) plotted here in terms of hand angle. On learning trials, a hand angle of 30° implies that the cursor heads straight to the target, resulting in a direction error of 0. The dotted line indicates average generalization magnitude of the group that experienced 320 learning trials. (*B*) Comparison between group-level generalization magnitude (colored dots) and learning curves predicted by the model. All curves were scaled such that their value on the 320th trial matched the group-averaged generalization magnitude of the 320 learning trial group (17). Thus, the fast learning curve was scaled up, while the net learning curve was scaled down. Likewise, the slow curve was scaled down by a very small amount to align the values. (*C*) Association of the fast state, slow state, and net learning reached at the end of different learning trial sets with generalization magnitude. There was a strong linear relationship ($r^2 = 0.95$) between generalization magnitude and level of the slow process (*Right*). This association was nonlinear for the fast process (*Middle*) and total learning (*Left*).

compared not just to participants who received sham hd-tdcs over left PPC ($P = 0.026$), but also those who received real stimulation over the right PPC ($P = 0.026$). Importantly, the right PPC stimulation group did not differ from the group that received sham stimulation over the same region ($P = 0.575$). Additional permutation tests ($n = 10{,}000$) confirmed this pattern by revealing a substantial effect of left PPC stimulation on the slow learning rate compared to sham ($P = 0.0042$) as well as right PPC stimulation ($P = 0.0052$) groups (Fig. 4*E*). Thus, left PPC disruption resulted in an inability to learn beyond the initial stages of exposure to the perturbation, when the slow process began to contribute. Indeed, in a model-free analysis, we found no group differences in average error during the first 25 learning trials ($F_{3,60} = 2.0976$, $P = 0.11$, $\eta^2_p = 0.094$; Fig. 4*F*), but error on the remaining trials was significantly larger in the left PPC hd-tdcs group ($F_{3,60} = 7.4094$, $P = 0.0003$, $\eta^2_p = 0.2703$; Fig. 4*F*) compared to the sham ($P = 0.0004$) and right stimulation groups ($P = 0.0141$). This selective deficit is in line with our recent findings in apraxic patients who had maximum lesion overlap in inferior parietal cortex (29), and likely reflects an inability to encode new information via the slow process rather than a failure to compute errors that drive learning; the latter would be expected to produce deficits during the early learning phase as well.

PPC Stimulation after Learning Blocked Generalization across Effectors. The results of our first two experiments suggested that 1) motor memories built via the slow learning mechanism are effector-independent since they strongly predict generalization across effectors and 2) disrupting left PPC blocks the encoding of memories built via this mechanism. A decisive test of this scheme is that interfering with left PPC activity after learning should disrupt generalization across effectors. We tested this in our third experiment in which we delivered cathodal hd-tdcs over PPC immediately after learning (Fig. 5*A*). We first confirmed that there were no differences between the real and sham stimulation groups either during the early ($F_{1,22} = 2.1022$, $P = 0.1612$, $\eta^2_p = 0.087$) or late ($F_{1,22} = 0.6317$, $P = 0.4352$, $\eta^2_p = 0.0279$) learning stages before the stimulation was delivered (Fig. 5*B*). However, poststimulation, clear group differences in generalization were evident. While significant generalization was observed in the sham group, it was absent in participants who received stimulation over PPC ($F_{1,44} = 16.1066$, $P = 0.0002$, $\eta^2_p = 0.268$). Direction errors on generalization trials (Fig. 5*C*) were significantly larger in the PPC stimulation group ($F_{3,40} = 20.9528$, $P < 0.0001$, $\eta^2_p = 0.611$) relative to sham ($P < 0.0001$) as well as additional "control" participants who received cathodal hd-tdcs over left M1 after learning ($P < 0.0001$). Furthermore, there was no difference between the sham and M1 stimulation groups ($P = 0.2153$), indicating that generalization occurred despite M1 disruption. This indicated that the lack of generalization in the PPC stimulation group was not due to any nonspecific effects of hd-tdcs. Interestingly, errors of the PPC stimulation group were not different from those of another control group that only underwent 40 trials of naïve learning ($P = 0.2634$). Moreover, the pattern of error reduction of the PPC hd-tdcs participants on generalization trials was qualitatively not different compared to this naïve group (Fig. 5*D*); it was as if the PPC stimulation group was learning afresh. Thus, disrupting the PPC (but not M1) impeded generalization, providing direct evidence for its causal role in representing an effector-independent memory trace.

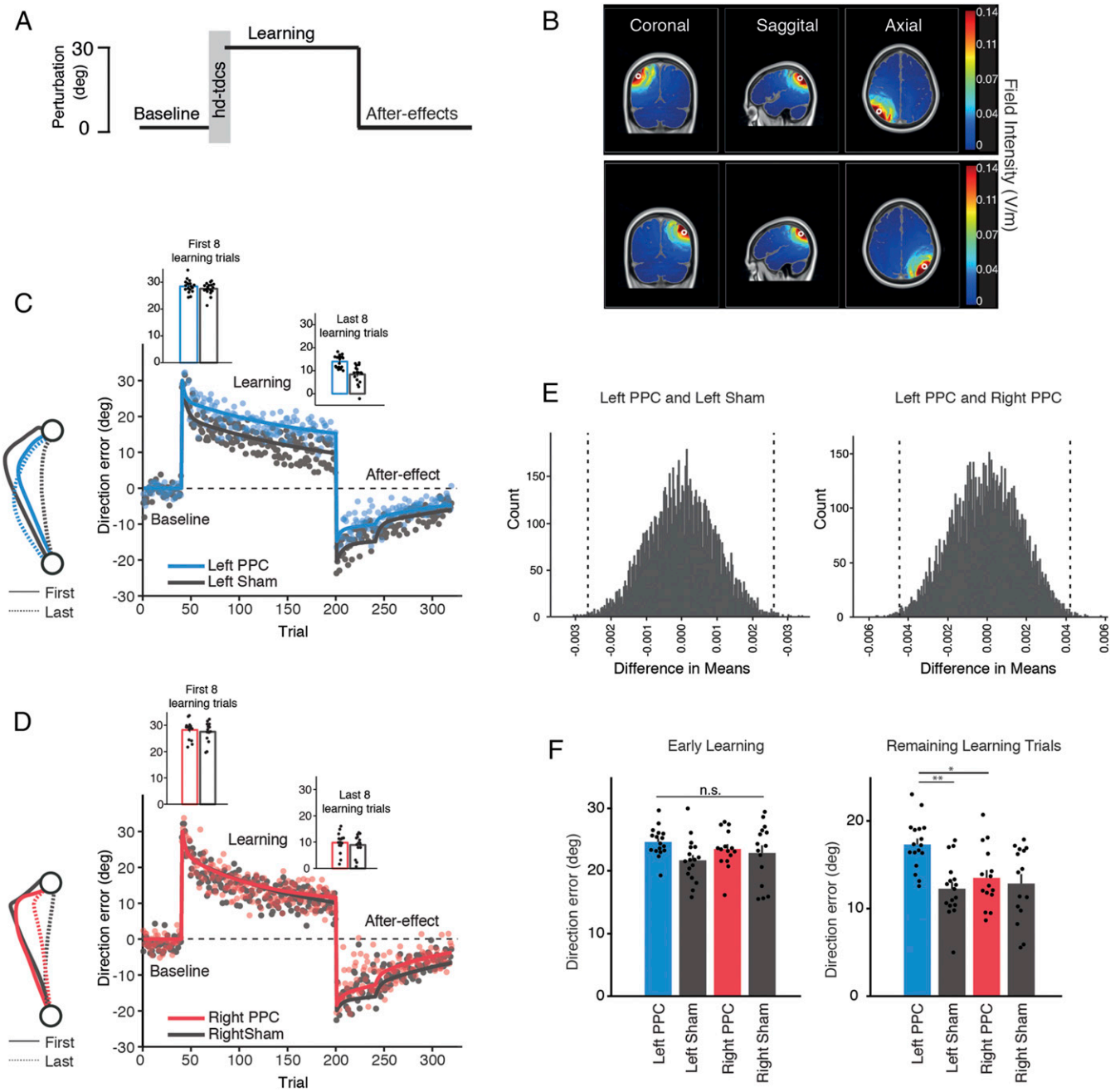

Fig. 4. Parietal hd-tdcs impairs slow process-mediated learning. (*A*) Baseline trials were followed by a learning block and an after-effects block. Cathodal hd-tdcs (2 mA, 15 min) was applied after baseline trials over PPC near the intraparietal sulcus (P3 or P4 locations; P3, $n = 17$ real, 17 sham; P4, $n = 15$ real, 15 sham). (*B*) Simulated distribution of electric fields with the hd-tdcs cathode over P3 (*Top*; cortical MNI, −41,−69, 45) and P4 (*Bottom*; cortical MNI, 41,−69, 44). Simulations (HD Explore; Soterix Medical) revealed an intensity of 0.167 V/m and 0.156 V/m at P3 and P4, respectively. (*C* and *D*, *Left*) Cursor trajectories of representative participants receiving real or sham hd-tdcs for the straight-ahead target from the first and last bins. (*Right*) Group-averaged direction error for each trial. Solid lines in these plots represent the predicted direction errors simulated using the mean values of the parameters obtained by fitting the multirate model to each participant's data. Inset bar plots show mean ± SEM direction error on the first and last eight learning trials. Dots in the bar plots indicate individual participants. (*E*) Distribution of the test statistic (difference in mean B_s value) for 10,000 permutations of data of the indicated groups. The vertical dotted lines represent the observed difference in means. (*F*) Mean ± SEM direction error during early learning (first 25 trials; *Left*) and remainder of the learning block (*Right*). Dots represent individual participants (*$P = 0.0141$, **$P < 0.001$).

Discussion

Developing motor memories through learning affords immense benefits in motor control. Even though it has been widely acknowledged that learning with one effector leads to the development of a motor memory that comprises component representations that are effector-independent, an understanding of how they are encoded in the brain has remained elusive. We demonstrate that effector-independent memory components are forged via a gradually evolving, implicit learning mechanism within areas that include the left PPC.

Our results challenge past work that has suggested that such representations are built via "algorithmic," or fast, strategic

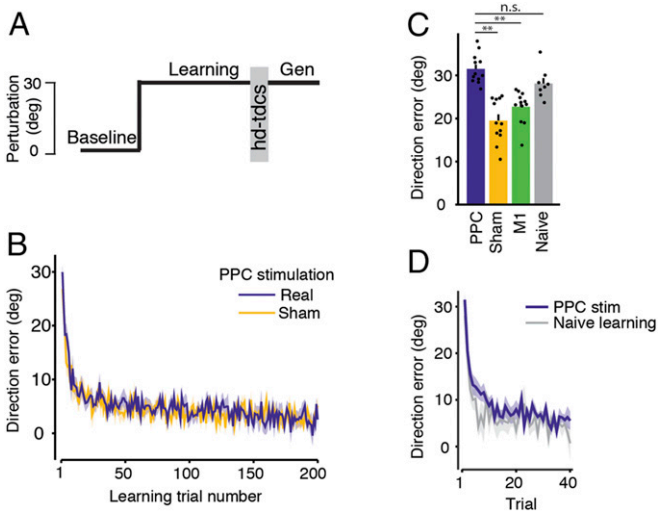

Fig. 5. Parietal hd-tdcs following learning blocks generalization. (*A*) Baseline trials were followed by a block of rotation learning trials. Cathodal hd-tdcs (2 mA, 15 min) was delivered after the learning block, followed by a test of generalization to the opposite arm. (*B*) Direction errors across learning trials for the real ($n = 12$) and sham ($n = 12$) PPC hd-tdcs groups. Shaded regions are SEM. (*C*) Mean ± SEM direction error on generalization trials for the real and sham PPC and real M1 ($n = 12$) hd-tdcs groups, shown with the mean error on the first learning trial of a group that only underwent naïve learning ($n = 8$). Dots represent individual participants. (*D*) Change in direction error over generalization trials for the real PPC hd-tdcs group. Also shown is the change in direction error during the learning block for the group that only underwent naïve learning. Shaded regions are SEM. ns, not significant (**$P < 0.0001$).

mechanisms that contribute to motor adaptation (10, 14). This is supported by the observation that generalization across effectors, the behavioral manifestation of an effector-independent representation, was most strongly predicted by the level of the gradual but not the fast process. This is also bolstered by the finding that generalization was absent in participants whose learning, in all likelihood, was principally driven by the fast process (those who trained only for 40 trials). These results suggest that the error-sensitive fast process contributes little to the acquisition of an effector-independent memory. This appears intuitive in that a strategic solution developed for one effector may not necessarily work for another. For example, countering an error with the left arm using a strategy such as "move away from the body midline" would exaggerate errors if this strategy is also used with the right arm. A more optimal solution could be to form representations that yield more robust predictions about the effects of the perturbation that induces the errors, which can then be accessed by untrained effectors. This can be achieved via the slower mechanisms that enable the recalibration of internal motor representations when faced with a perturbing environment. This is not to say, however, that fast, strategic processes do not drive learning or contribute to the encoding of motor memories. Learning has been shown to occur even with very brief exposure to visuomotor rotations like the one we have used; such learning, in all probability, is driven by a fast, explicit process. This kind of learning, however, appears to subserve a latent memory that is expressed as savings, or faster adaptation, when the same effector is reexposed to the original learning conditions (30). It remains to be established whether memory components encoded by this fast process during motor adaptation are only effector-specific; our finding of the absence of generalization when learning is driven by the fast process (40 learning trial group) would imply so. This dissociation could be tested in a fresh series of studies in the future.

A pertinent question is whether effector-independent memory components can be formed simply by repeated practice rather than the slow process per se. A couple of observations suggest that this is unlikely to be the case. First, the magnitude of generalization appeared to saturate with extended practice. Specifically, errors on generalization trials after 320 learning trials were not substantially lower than after 160 learning trials, even though the amount of practice doubled. This leveling off mirrored the saturation in the slow process as the number of learning trials increased. This should not have been the case, i.e., generalization should have continued to increase if movement repetition promoted generalization beyond levels contributed by this mechanism. Second, recent work suggests that extended practice or experience does not influence the rate of implicit learning, nor the magnitude of aftereffects in motor adaptation (31). Rather, repetition results in caching of stimulus–response associations that trigger faster retrieval upon reexposure to previously learned contexts. Thus, it appears that repetition provides no additional benefit for implicit learning or phenomena associated with implicit learning such as aftereffects, and, as we suggest here, generalization to other effectors.

What is the nature of the effector-independent memory components that facilitate intereffector generalization? In our case, these are unlikely to be representations of muscle activation patterns or muscle synergies acquired during learning. Rather, a strong possibility is that these are abstract representations of the relationship between the motion of an effector and its sensory consequences, i.e., tacit knowledge about how the arm movement should be directed in order to make the cursor go straight to the displayed target in the face of the perturbation. Critically, such representations are continuously calibrated via implicit learning (32) and ensure that the planned and executed movement trajectories are identical in visual space. This idea, however, leads to the intriguing question of whether any new, higher-level representation that ensures correspondence between planned and actual motion of an effector to satisfy the action goal also facilitates generalization across effectors. We believe that this is likely to be the case. For example, in tasks that require learning of novel motor coordination patterns, an acquired representation of a generic temporal relationship of movements of different effectors may best account for generalization to untrained effectors (33). Likewise, representations of abstract visuospatial associations during sequence learning are likely to underlie generalization of the learned sequence to other effectors (34). The mechanism that underpins the development and updating of these representations could provide the gateway for such generalization.

The notion that higher-level, abstract representations act as a scaffold for generalization also resonates with recent suggestions made in the perceptual learning literature. Early studies considered visual perceptual learning to be specific to a trained retinal location, which was explained using a framework in which learning-related plasticity occurred only in early visual cortical areas (35). However, more recent work has demonstrated generalization across locations (36), which, critically, can be accounted for by the inclusion of higher-level, location-invariant representations in a computational architecture of perceptual learning (37). Likewise, generalization across stimulus orientations can been explained using a rule-based conceptual model in which higher-order brain areas learn the rules of reweighting inputs from early visual cortex (38). Interestingly, such representations seem to evolve in nonretinotopic regions such as lateral intraparietal area, as shown in tasks that require motion discrimination learning (39). Analogous conclusions can be drawn from studies probing generalization of speech (40) and tactile perceptual learning (41). While these studies do not examine a different effector per se, the idea that generalization to any untrained condition is likely driven by a broader, higher-level representation suggests that this may be a fundamental principle across many learning systems.

Past work has emphasized that memories acquired via error-driven learning are encoded primarily in M1 (19, 20). Branching

off from this line of thought, we demonstrate a role for the PPC in the encoding of motor memories. This mirrors seminal new results that have uncovered encoding of other forms of systems memory in PPC (42), and more broadly, aligns with recent work highlighting critical contributions of nonmotor regions to the memory of motor acts (43). Our findings also lend causal support to imaging studies that have demonstrated overlapping activity in intraparietal regions when different effectors are moved, presumably reflecting the presence of effector-independent motor representations (22, 23). Yet, the result that PPC causally contributes to the formation of such memories should not be taken to imply that M1 does not encode motor memories at all. There is ample evidence, even down to the single neuron level (44), that M1 can hold motor memories. We posit, though, that components of motor memories encoded in M1 may be more strongly tied to a particular effector and include, for instance, lower-level representations of task-related muscle activity patterns or specific motor responses. This plausible dissociation—effector independence of PPC and effector specificity of M1 representations—could also then explain why modulation of M1 does not affect generalization across effectors (21), but its disruption leads to poor retention of learning when tested with the same effector as is used to learn (20). Indeed, some areas of PPC that show overlapping activity when different effectors are moved project to effector-specific regions in M1 (24), an organization that may provide the neurophysiological foundation for such effects.

How might the PPC participate in memory encoding? One possibility is that the PPC computes the errors that drive learning and memory formation. However, this is less likely in our case because PPC disruption did not impede the error-sensitive fast process, which in fact acts when the error is large. Additionally, in our third experiment, there was no learning impairment during the brief generalization period following PPC stimulation; a compromise in error computation should potentially have produced one. This raises the possibility that computation of the error that drives learning in our task may occur outside the PPC; the cerebellum (45) and/or frontal areas such as premotor cortex or even M1 (46) could be plausible candidates. A second, more likely possibility is that the effector-independent component of the memory is built in PPC or a network that includes PPC as a critical substrate. This thought aligns with the putative role of the PPC in holding more abstract action plans (47) and "functional" memory structures (48, 49). For instance, the evolution of generic visuospatial associations during sequence learning is closely tied to an increase in activity in the (left) inferior parietal cortex, and, notably, this activity remains high as the sequence is replayed with different effectors (48). Our finding that generalization across effectors is blocked after postlearning disruption of areas near the inferior parietal cortex is in harmony with these results. Such an arrangement could reflect an efficient coding scheme in which a common neuronal population is engaged for relatively similar movements of different effectors. The notion that effector-independent components may be encoded within PPC is also in line with some very interesting recent findings in dysplasic individuals in whom the plastic evolution of memory representations of object manipulation with the feet (due to the loss of the arms) occurs in intraparietal areas (50). A relevant question, though, is whether the PPC possesses the neurophysiological foundations to actually encode a memory. Findings of tuning of directional selectivity in medial intraparietal regions following motor adaptation (51), as well as simulations in which generalization patterns are produced by updating weights between parietal-like narrow Gaussian-tuned visual units and motor units (52), suggest that this is likely the case.

Our results also reveal a striking asymmetry in generalization and left-laterality of the PPC contributions; these could be related effects. We suggest that this occurs not because a learning mechanism is tied to a particular effector, but because motor representations built through implicit learning are lateralized largely to left brain hemisphere, independent of the effector used to learn. Indeed, the left hemisphere in right-handers possesses a capacity for motor learning and memory that is distinct from the right. For instance, adaptation deficits are more common with left than right hemisphere damage (53), and skill learning is more enhanced after left than right hemisphere facilitation by brain stimulation (54). Imaging studies have identified neural correlates of sequence learning (48), real and imagined tool-use actions (55), and well-learned gestures (56) that are left-lateralized. Relatedly, studies in apraxic (57) and other patients (58) have shown that left hemisphere damage, specifically around the left intraparietal sulcus, results in behavioral deficits that reflect loss of knowledge of learned transitive and intransitive actions. These findings collectively suggest that representations of implicitly learned, complex actions are asymmetrically organized: they are much stronger in the left hemisphere compared to the right. As such, the right but not always the left arm has direct access to these representations, which could produce the asymmetric generalization behaviorally as and when these representations are updated. Why such a lateralized system evolved in humans remains an open question, but it is possible that, over the course of evolution, such an architecture enabled the accommodation of increased motor complexity without significant expansion of neural tissue.

In conclusion, our results provide insight into the mechanism by which effector-independent representations of a motor memory are encoded and provide causal evidence that this encoding occurs in areas that include the left PPC, but not necessarily M1. The availability of such representations in "association" regions known to be important for higher-order aspects of movement such as intention and decision-making (59) likely reflects the evolutionary emergence of an efficient neural architecture. Such an organization could facilitate more optimal movement planning in the brain by enabling the specification of certain movement parameters independent of the effector used to execute an action.

Materials and Methods

Participants. A total of 180 young, healthy right-handed individuals (age 18 to 27 y, 45 females) participated across various main and control experiments of this study. The distribution of subjects across different groups in the experiments is given in subsequent sections. Subjects were included if they reported no neurological condition, cognitive impairment, or orthopedic injuries. Experimental protocols were approved by the institute ethics committee of the Indian Institute of Technology Gandhinagar, and participants gave written informed consent prior to participation.

Apparatus. Participants sat facing a large digitizing tablet and used a handheld stylus to make reaching movements on it. Direct vision of the hand was blocked by means of a mirror mounted above the tablet. A start circle and targets for the reach were displayed on an HDTV placed horizontally above the mirror. Although direct vision of the hand was not available, feedback about hand position was displayed on the screen by means of a cursor. The start position, targets, and cursor were all reflected onto the mirror, and participants looked into the mirror while moving. Cursor feedback could be veridical or manipulated in different ways relative to actual hand motion.

Experimental Design and Task Procedure. To begin a trial, participants brought the cursor into the start circle and were presented with the target and an audiovisual "go" signal 500 ms later. They were instructed to make fast and accurate movements, and received performance feedback on each trial through a numerical score based on movement accuracy. This score was not analyzed.

Experiment 1. Participants in experiment 1 (n = 64) performed 10-cm-long movements from a start position to a target placed straight ahead under continuous cursor feedback. After a few familiarization movements, participants performed baseline trials with their left and their right arm (16 trials with each arm, counterbalanced) on which cursor and hand motion was matched. Following baseline, participants performed learning trials on which motion of the cursor was rotated 30° counterclockwise relative to hand motion. Critically, participants differed in terms of the arm used to

learn and also the number of learning trials experienced. Half the participants ($n = 32$) learned with their left arm, while the remaining used their right arm to learn. Additionally, within each left or right arm group, participants experienced either 40, 80, 160, or 320 learning trials ($n = 8$ each). Following learning, all participants were exposed to the same rotation with the opposite arm for a fixed set of 40 trials to test for generalization.

The X–Y hand position data were low-pass Butterworth-filtered with a 10-Hz cutoff frequency. Position data were differentiated to yield velocity values. Our primary measure of interest was direction error, which was calculated for each trial as the angle between the line joining the start circle and the target and the line joining the start circle and the cursor position at peak velocity. The mean baseline direction error of the corresponding arm for each participant was subtracted from the direction error on learning trials for that participant, and learning was quantified as a reduction in this direction error across learning trials. Further, performance upon initial exposure to the rotation and end of learning was quantified as the mean direction error on the first and last four learning trials respectively.

To assess generalization, we compared the direction error on the first naïve learning trial of an arm to that observed on the first generalization trial of the same arm. Using only the first trial for this comparison was absolutely critical because subsequent trials in the generalization block allow the untrained limb to learn, thereby contaminating the generalization measure. Generalization was thus determined by probing, for instance, whether direction errors for participants that learned naively with the right arm were different from those of participants who used the right arm after they had learned with the left arm. Smaller errors with the right arm on generalization trials would indicate generalization from the left arm to the right. A similar approach was taken for determining generalization from the right arm to the left. Thus, our comparisons were always within the same arm and at the same time point, yielding a more "pure" measure of generalization, since potential confounds related to handedness or baseline performance differences between the arms were avoided. The magnitude of generalization for each trial set was calculated as the difference in the group-averaged direction error of the naïve learning and generalization trials. Note that, while this is a better measure of generalization, it is not a "within-participant" measure since the same arm of different participants is compared. For completeness, we also calculated left to right arm generalization magnitude for individual participants as: (left arm errors on naïve learning trials – right arm errors on generalization trials)/left arm error on naïve learning trials. This was then expressed as a percentage by multiplying by 100. Again, only the first naïve learning and generalization trials were used in this calculation.

Computational Model. In order to understand the relationship between the mechanisms that drive learning and the observed generalization, we considered a multiprocess learning framework in which learning is driven by a fast, explicit process that operates in parallel with a slower implicit process, both of which are error-sensitive (3, 5). We simulated the learning patterns that would emerge from this framework using the following equations:

$$e(n) = x(n) + u(n)$$

$$x(n) = x_s(n) + x_f(n)$$

$$x_s(n+1) = A_s * x_s(n) + B_s * e(n)$$

$$x_f(n+1) = A_f * x_f(n) + B_f * e(n),$$

where $e(n)$ is the error experienced on the nth trial, $x(n)$ is the net motor output on the n^{th} trial, $u(n)$ is perturbation imposed on the n^{th} trial, x_s and x_f are internal slow and fast states, A_s and A_f are retention factors for the slow and fast processes, and B_s and B_f are the slow and fast learning rates, respectively.

The parameters used for the simulation were derived by fitting this model to the trial-by-trial learning data using the fmincon function in Matlab, with A_s constrained to be greater than A_f, and B_s smaller than B_f. Our results indicated that generalization occurred only from the left arm to the right, and so only the left arm naïve learning data ($n = 32$) were used for model fitting. We created 10,000 bootstrapped data samples, each as the average of 32 random choices made from the set of 32 participants with replacement, and then fit the model to these samples. Median parameter values resulting from the fit were: $A_s = 0.998$, $A_f = 0.896$, $B_s = 0.0161$, and $B_f = 0.255$. These values were used to simulate the slow, fast, and total learning curves (Fig. 3*A*). We then investigated whether the amount of generalization was most strongly associated with the level of the slow process, fast process, or total learning at the end of different learning trial sets.

Additional Experiment for Model Parameter Estimation. There is no "gold standard" perturbation protocol to obtain model parameters. To test the robustness of the association between generalization and the underlying learning processes, however, we performed another experiment with a different perturbation protocol and estimated the model parameters by fitting the multirate model to the learning data from this experiment. Our goal was to determine whether the generalization seen in experiment 1 could be predicted by the fast or slow states or total learning derived by fitting the model to data from a completely different experiment.

A new set of participants ($n = 8$) performed a block of 40 baseline movements of 10 cm length. They were then exposed to a 30° counterclockwise cursor rotation for a block of 200 trials, which was followed by an opposite (clockwise) rotation of the same magnitude for a brief set of 20 trials. Following this, participants experienced a block of 80 "error-clamp" trials wherein the visual errors were clamped to zero by fixing the motion of the cursor in the direction of the target regardless of the direction of hand motion. Only the left arm was used in this task. Behaviorally, this kind of perturbation protocol results in a phenomenon termed "spontaneous recovery" (3) where, on the error-clamp trials, the hand moves in a direction that is appropriate for compensating the originally imposed, longer-duration perturbation (counterclockwise rotation in our case). This rebound toward the originally learned behavior reflects the effects of a lingering slow process (the fast process gets reset to zero following the brief exposure to the counter perturbation and does not change after that in the error clamp; however, the slow process is slower to decay and does not reach zero in the same time). Thus, this "A-B-error clamp" perturbation schedule allows the estimation of the slow component independent of the faster one.

Data processing and computation of various dependent variables remained similar to before. We again bootstrapped the data to create 10,000 samples, each as the average of 8 random selections made from the set of 8 participants with replacement, and fit the multirate learning model to them. Median parameter values that we obtained were $A_s = 0.998$, $A_f = 0.887$, $B_s = 0.031$, and $B_f = 0.165$. We used these parameter values to simulate the fast and slow states as well as the net motor output. Finally, we probed whether the generalization seen in experiment 1 was best predicted by levels of these newly simulated slow or fast states.

Experiment 2. The results of experiment 1 indicated that generalization across effectors was most strongly associated with the slow learning process. In experiment 2, we probed whether disrupting the posterior parietal cortex (PPC) would specifically impede this process. The setup and general task conditions for experiment 2 remained similar to experiment 1. Briefly, participants ($n = 64$) made reaching movements from a start position to one of eight targets placed around the edge of an imaginary circle at a radial distance of 15 cm with either their left ($n = 30$) or their right arm ($n = 34$). After performing 40 baseline reaches, participants were exposed to a 30° counterclockwise rotation of the cursor for 160 trials, which was then followed by an after-effects block of 120 trials. Cursor feedback was withheld for the first 40 after-effects trials, whereas, in the remaining 80 trials, the cursor was redisplayed on the screen with its motion matched to the hand. Each target was displayed once on each "bin" (set of eight consecutive trials) during the baseline and learning blocks; in the after-effects block, one randomly selected target was displayed twice in a bin while a different one was not displayed. Unlike experiment 1, the opposite arm was not tested, since this experiment was not designed to test generalization. The behavioral measure of interest continued to be direction error, which was calculated as explained earlier. Early and late learning performance was quantified as the mean direction error on the first and last eight learning trials (one movement to each of the eight targets). Learning was characterized by a reduction in the (baseline un-subtracted) direction error over trials.

High-Definition Transcranial Direct Current Stimulation (hd-tdcs). In this experiment (and in experiment 3), we delivered cathodal hd-tdcs over the PPC. Cathodal, and not anodal, stimulation was used primarily for two reasons: first, it produces more stable inhibitory effects on motor learning (60), which was aligned with our goal of disrupting PPC processing rather than enhancing it. Second, anodal stimulation is known to produce more heterogenous behavioral effects (61, 62). We used a 4 × 1 hd-tdcs device (Soterix Medical) with Ag/AgCl sintered ring electrodes of 1.2 cm outer diameter and 0.6 cm inner diameter. Electrodes were arranged in a ring configuration with the cathode as the central electrode and the other four electrodes (anodes) forming a ring around it. The area of cortex undergoing stimulation is far more restricted in this configuration than the conventional two-electrode configuration (63). It has also been shown that the current does not spread substantially outside the stimulation area when a 4 × 1 ring

configuration is used, with the electric field falling below 30% of the peak at the ring perimeter (64).

For participants who used their right arm to learn, stimulation was applied over the left PPC, while, for those who learned with their left arm, the right PPC was stimulated. The location of the PPC was determined using the 10–20 EEG system. The P3 and P4 locations, which are in close proximity to the intraparietal sulcus (65, 66), were chosen as the stimulation sites. The cathode was placed at the P3 location for the left hemisphere stimulation participants, which corresponded to MNI coordinates of (−52, −80, 54) on a physical model of the ICBM-152 head and (−41, −69, 45) on the cortex (67). The anodes were arranged in the P1, P5, CP3, and PO3 locations. For right hemisphere stimulation, the cathode was placed at the P4 location [MNI coordinates of (53, −80, 54) on the ICBM-152 head, (41, −69, 44) on the cortex], while the anodes were placed at the P2, P6, CP4, and PO4 locations. All electrodes were held in place via a tight-fitting cap with plastic electrode holders filled with conductive electrolyte gel to improve contact quality.

All participants were readied for hd-tdcs before the baseline block. For the groups receiving real hd-tdcs (left hemisphere PPC, $n = 17$; right hemisphere PPC, $n = 15$), the current magnitude was set at 2 mA and stimulation was administered for 15 min. Delivery of hd-tdcs started immediately after the baseline block of trials. Participants sat quietly for the first 10 min of the stimulation, while the last 5 min of stimulation overlapped with the early portion of the learning block. Participants continued to perform the learning trials uninterrupted after the stimulation ended; the entire task after the end of stimulation took about 20 to 25 min. The same procedures were followed for participants that received sham PPC stimulation (left hemisphere, $n = 17$; right hemisphere, $n = 15$). However, for them, the current rose to 2 mA over 30 s and then dropped to zero over the next 30 s, thereby ensuring that they felt the "tingling" sensation associated with the stimulation. Participants were unaware of the group they were in, and reported no discomfort later.

Model Fitting. We fit the multirate learning model to the trial-by-trial learning data separately for each participant in the four groups (real/sham stimulation over left/right PPC). Fitting the model to individual participant data was essential in this experiment because we could not assume uniform effects of hd-tdcs across participants, and we wished to obtain unbiased parameter estimates. The constraints on the parameters remained similar to experiment 1 ($A_s > A_f$ and $B_f > B_s$). Further, for the first 40 trials of the aftereffects block, the error term was set to zero since there was no visual feedback on these trials, and thus no visual error to (re)learn from. To better ensure identification of least squared error and assess the sensitivity of the fits to the initial conditions, we used 180 different starting value combinations for the parameters. We found very consistent fits within the constrained parameter space. Mean parameter values for the various groups are in *SI Appendix*, Table S1.

Experiment 3. Experiment 3 ($n = 32$) was designed to test whether generalization could be impeded if the PPC was disrupted postlearning. The setup and general task conditions remained same as earlier. Briefly, participants made 10-cm-long reaches from a start position to a target in the straight-ahead direction under continuous feedback of hand position. Participants were randomly divided into three groups. Two of the three groups learned to compensate a 30° counterclockwise rotation of the feedback cursor over 200 trials with their left arm. Participants in the third, "naïve" group learned the rotation with their right arm for 40 trials. Participants in the first two groups received real ($n = 12$) or sham ($n = 12$) cathodal hd-tdcs over PPC, while the naïve group ($n = 8$) did not receive any stimulation. Following hd-tdcs delivery, participants in the stimulation groups performed 40 trials with their right arm to test for the effects of hd-tdcs on generalization from prior left arm learning. The behavioral measure of interest again was direction error. Quantification of learning and generalization was similar to experiment 1.

hd-tdcs Protocol. The setup and procedures for hd-tdcs remained largely identical to experiment 2. Stimulation was delivered in a 4 × 1 ring arrangement over the P3 location with a current magnitude of 2 mA and duration of 15 min. hd-tdcs started immediately after completion of the learning block, and participants sat quietly during stimulation. For the sham group, setup procedures remained the same, but the current rose to 2 mA over 30 s and then dropped to zero over the next 30 s. Participants did not know which group they were in and reported no discomfort with the hd-tdcs.

Control Experiment for Nonspecific hd-tdcs Effects. We recruited another group of participants ($n = 12$) for a control experiment that involved delivery of cathodal hd-tdcs over left M1. This was done to control for any potential nonspecific effects of active hd-tdcs. This also allowed us to test whether M1 causally influences generalization. The current intensity and duration for this group were also set at 2 mA and 15 min, respectively. The task for this group of participants remained identical to the group that received hd-tdcs over PPC. In other words, these participants also learned to compensate for a 30° counterclockwise visuomotor rotation for 200 trials with their left arm, were administered the hd-tdcs postlearning, and were then tested for generalization using their right arm (40 trials). Data from these participants were analyzed along with those obtained from participants in experiment 3.

Data Removal. Trials on which participants failed to initiate a movement, lifted the stylus off the digitizer leading to loss of data, or moved in a direction drastically different from the target direction were excluded from the analysis. Across all participants in the entire study, 1.1% of the trials were removed.

Statistics. We typically used analysis of variance (ANOVA) to test for main or interaction effects of various factors on the dependent kinematic variables of interest (primarily the direction error). Assumptions of normality required for ANOVA were tested using Shapiro–Wilk tests. In experiment 1, group and trial set differences in learning were assessed by subjecting direction errors to a two-way ANOVA. Generalization was analyzed statistically using another two-way ANOVA with block (learning/generalization) and trial set as factors. Early and late learning differences across various hd-tdcs groups of experiments 2 and 3 were compared using one-way ANOVAs. One-way ANOVA was also used for assessing generalization differences between the groups of experiment 3. Tukey's post hoc tests, which adjust for multiple comparisons, were performed when main or interaction effects were significant. Partial eta-squared (η^2_p) values were calculated for effect sizes.

In experiment 2, we also examined if the parameters derived from the model fitting procedure (A_s, A_f, B_s, and B_f) differed across the four hd-tdcs groups (real/sham over left/right PPC) using the Kruskal–Wallis test. Post hoc pairwise comparisons were done using the Wilcoxon rank-sum test corrected for multiple comparisons via the Benjamini–Hochberg method. Specific group differences were also confirmed using permutation tests ($n = 10{,}000$), which evaluate the (null) hypothesis that the score for each participant is independent of the group they are in. For this, the difference in mean parameter values of the groups being compared was used as the test statistic. The proportion of times that the difference in means in the distribution obtained from the permutation procedure exceeded the originally observed difference was calculated in order to test the null hypothesis. The significance threshold was set at 0.05 for all statistical tests.

Data Availability. Data supporting the findings of the study are available on Figshare at https://figshare.com/articles/Kumar_et_al_2020_data/12416426.

ACKNOWLEDGMENTS. We thank Bhoomika Sonane for assistance with data collection and IIT Gandhinagar for laboratory facilities. This work was supported by the Ramanujan Fellowship and grants from the Health Sciences Committee and the Cognitive Science Research Initiative of the Department of Science and Technology (all of the Government of India) to P.K.M.

1. P. M. Fitts, M. I. Posner, *Human Performance*, (Brooks/Cole Pub. Co., Belmont, CA, 1967).
2. G. Logan, Toward an instance theory of automatization. *Psychol. Rev.* **95**, 492–527 (1988).
3. M. A. Smith, A. Ghazizadeh, R. Shadmehr, Interacting adaptive processes with different timescales underlie short-term motor learning. *PLoS Biol.* **4**, e179 (2006).
4. J. Y. Lee, N. Schweighofer, Dual adaptation supports a parallel architecture of motor memory. *J. Neurosci.* **29**, 10396–10404 (2009).
5. S. D. McDougle, K. M. Bond, J. A. Taylor, Explicit and Implicit Processes Constitute the Fast and Slow Processes of Sensorimotor Learning. *J. Neurosci.* **35**, 9568–9579 (2015).
6. P. Alvarez, L. R. Squire, Memory consolidation and the medial temporal lobe: A simple network model. *Proc. Natl. Acad. Sci. U.S.A.* **91**, 7041–7045 (1994).
7. Y. Yotsumoto, L. H. Chang, T. Watanabe, Y. Sasaki, Interference and feature specificity in visual perceptual learning. *Vision Res.* **49**, 2611–2623 (2009).
8. F. A. Hellebrandt, Cross education; ipsilateral and contralateral effects of unimanual training. *J. Appl. Physiol.* **4**, 136–144 (1951).
9. H. G. Taylor, K. M. Heilman, Left-hemisphere motor dominance in righthanders. *Cortex* **16**, 587–603 (1980).
10. J. Wang, R. L. Sainburg, Mechanisms underlying interlimb transfer of visuomotor rotations. *Exp. Brain Res.* **149**, 520–526 (2003).

11. J. W. Krakauer, P. Mazzoni, A. Ghazizadeh, R. Ravindran, R. Shadmehr, Generalization of motor learning depends on the history of prior action. *PLoS Biol.* **4**, e316 (2006).
12. M. A. Perez *et al*., Neural substrates of intermanual transfer of a newly acquired motor skill. *Curr. Biol.* **17**, 1896–1902 (2007).
13. N. Kumar, A. Kumar, B. Sonane, P. K. Mutha, Interference between competing motor memories developed through learning with different limbs. *J. Neurophysiol.* **120**, 1061–1073 (2018).
14. N. Malfait, D. J. Ostry, Is interlimb transfer of force-field adaptation a cognitive response to the sudden introduction of load? *J. Neurosci.* **24**, 8084–8089 (2004).
15. J. A. Taylor, G. J. Wojaczynski, R. B. Ivry, Trial-by-trial analysis of intermanual transfer during visuomotor adaptation. *J. Neurophysiol.* **106**, 3157–3172 (2011).
16. J. Wang, M. Joshi, Y. Lei, The extent of interlimb transfer following adaptation to a novel visuomotor condition does not depend on awareness of the condition. *J. Neurophysiol.* **106**, 259–264 (2011).
17. W. M. Joiner, M. A. Smith, Long-Term Retention Explained by a Model of Short-Term Learning in the Adaptive Control of Reaching. *J. Neurophysiol.* **100**, 2948–2955 (2008).
18. J. Doyon, H. Benali, Reorganization and plasticity in the adult brain during learning of motor skills. *Curr. Opin. Neurobiol.* **15**, 161–167 (2005).
19. A. G. Richardson *et al*., Disruption of primary motor cortex before learning impairs memory of movement dynamics. *J. Neurosci.* **26**, 12466–12470 (2006).
20. J. M. Galea, A. Vazquez, N. Pasricha, J. J. de Xivry, P. Celnik, Dissociating the roles of the cerebellum and motor cortex during adaptive learning: The motor cortex retains what the cerebellum learns. *Cereb. Cortex* **21**, 1761–1770 (2011).
21. H. Block, P. Celnik, Stimulating the cerebellum affects visuomotor adaptation but not intermanual transfer of learning. *Cerebellum* **12**, 781–793 (2013).
22. M. Rijntjes *et al*., A blueprint for movement: Functional and anatomical representations in the human motor system. *J. Neurosci.* **19**, 8043–8048 (1999).
23. F. T. Leoné, T. Heed, I. Toni, W. P. Medendorp, Understanding effector selectivity in human posterior parietal cortex by combining information patterns and activation measures. *J. Neurosci.* **34**, 7102–7112 (2014).
24. T. Heed, F. T. Leone, I. Toni, W. P. Medendorp, Functional versus effector-specific organization of the human posterior parietal cortex: Revisited. *J. Neurophysiol.* **116**, 1885–1899 (2016).
25. H. Cui, R. A. Andersen, Posterior parietal cortex encodes autonomously selected motor plans. *Neuron* **56**, 552–559 (2007).
26. E. Premereur, P. Janssen, W. Vanduffel, Effector specificity in macaque frontal and parietal cortex. *J. Neurosci.* **35**, 3446–3459 (2015).
27. A. Tosoni, G. Galati, G. L. Romani, M. Corbetta, Sensory-motor mechanisms in human parietal cortex underlie arbitrary visual decisions. *Nat. Neurosci.* **11**, 1446–1453 (2008).
28. M. A. Nitsche *et al*., Level of action of cathodal DC polarisation induced inhibition of the human motor cortex. *Clin. Neurophysiol.* **114**, 600–604 (2003).
29. P. K. Mutha, L. H. Stapp, R. L. Sainburg, K. Y. Haaland, Motor adaptation deficits in ideomotor apraxia. *J. Int. Neuropsychol. Soc.* **23**, 139–149 (2017).
30. D. M. Huberdeau, A. M. Haith, J. W. Krakauer, Formation of a long-term memory for visuomotor adaptation following only a few trials of practice. *J. Neurophysiol.* **114**, 969–977 (2015).
31. D. M. Huberdeau, J. W. Krakauer, A. M. Haith, Practice induces a qualitative change in the memory representation for visuomotor learning. *J. Neurophysiol.* **122**, 1050–1059 (2019).
32. P. Mazzoni, J. W. Krakauer, An implicit plan overrides an explicit strategy during visuomotor adaptation. *J. Neurosci.* **26**, 3642–3645 (2006).
33. S. Vangheluwe, N. Wenderoth, S. P. Swinnen, Learning and transfer of an ipsilateral coordination task: Evidence for a dual-layer movement representation. *J. Cogn. Neurosci.* **17**, 1460–1470 (2005).
34. R. S. Bapi, K. Doya, A. M. Harner, Evidence for effector independent and dependent representations and their differential time course of acquisition during motor sequence learning. *Exp. Brain Res.* **132**, 149–162 (2000).
35. A. Karni, D. Sagi, Where practice makes perfect in texture discrimination: Evidence for primary visual cortex plasticity. *Proc. Natl. Acad. Sci. U.S.A.* **88**, 4966–4970 (1991).
36. L. Q. Xiao *et al*., Complete transfer of perceptual learning across retinal locations enabled by double training. *Curr. Biol.* **18**, 1922–1926 (2008).
37. B. A. Dosher, P. Jeter, J. Liu, Z. L. Lu, An integrated reweighting theory of perceptual learning. *Proc. Natl. Acad. Sci. U.S.A.* **110**, 13678–13683 (2013).
38. J. Y. Zhang *et al*., Rule-based learning explains visual perceptual learning and its specificity and transfer. *J. Neurosci.* **30**, 12323–12328 (2010).
39. C. T. Law, J. I. Gold, Neural correlates of perceptual learning in a sensory-motor, but not a sensory, cortical area. *Nat. Neurosci.* **11**, 505–513 (2008).
40. A. G. Hervais-Adelman, M. H. Davis, I. S. Johnsrude, K. J. Taylor, R. P. Carlyon, Generalization of perceptual learning of vocoded speech. *J. Exp. Psychol. Hum. Percept. Perform.* **37**, 283–295 (2011).
41. H. Dempsey-Jones *et al*., Transfer of tactile perceptual learning to untrained neighboring fingers reflects natural use relationships. *J. Neurophysiol.* **115**, 1088–1097 (2016).
42. S. Brodt *et al*., Fast track to the neocortex: A memory engram in the posterior parietal cortex. *Science* **362**, 1045–1048 (2018).
43. N. Kumar, T. F. Manning, D. J. Ostry, Somatosensory cortex participates in the consolidation of human motor memory. *PLoS Biol.* **17**, e3000469 (2019).
44. R. Paz, T. Boraud, C. Natan, H. Bergman, E. Vaadia, Preparatory activity in motor cortex reflects learning of local visuomotor skills. *Nat. Neurosci.* **6**, 882–890 (2003).
45. K. E. Cullen, J. X. Brooks, Neural correlates of sensory prediction errors in monkeys: Evidence for internal models of voluntary self-motion in the cerebellum. *Cerebellum* **14**, 31–34 (2015).
46. M. Inoue, M. Uchimura, S. Kitazawa, Error signals in motor cortices drive adaptation in reaching. *Neuron* **90**, 1114–1126 (2016).
47. D. L. Harrington *et al*., Specialized neural systems underlying representations of sequential movements. *J. Cogn. Neurosci.* **12**, 56–77 (2000).
48. S. T. Grafton, E. Hazeltine, R. B. Ivry, Abstract and effector-specific representations of motor sequences identified with PET. *J. Neurosci.* **18**, 9420–9428 (1998).
49. R. S. Bapi, K. P. Miyapuram, F. X. Graydon, K. Doya, fMRI investigation of cortical and subcortical networks in the learning of abstract and effector-specific representations of motor sequences. *Neuroimage* **32**, 714–727 (2006).
50. E. Striem-Amit, G. Vannuscorps, A. Caramazza, Plasticity based on compensatory effector use in the association but not primary sensorimotor cortex of people born without hands. *Proc. Natl. Acad. Sci. U.S.A.* **115**, 7801–7806 (2018).
51. S. Haar, O. Donchin, I. Dinstein, Dissociating visual and motor directional selectivity using visuomotor adaptation. *J. Neurosci.* **35**, 6813–6821 (2015).
52. H. Tanaka, T. J. Sejnowski, J. W. Krakauer, Adaptation to visuomotor rotation through interaction between posterior parietal and motor cortical areas. *J. Neurophysiol.* **102**, 2921–2932 (2009).
53. P. K. Mutha, R. L. Sainburg, K. Y. Haaland, Critical neural substrates for correcting unexpected trajectory errors and learning from them. *Brain* **134**, 3647–3661 (2011).
54. H. M. Schambra *et al*., Probing for hemispheric specialization for motor skill learning: A transcranial direct current stimulation study. *J. Neurophysiol.* **106**, 652–661 (2011).
55. J. Moll *et al*., Functional MRI correlates of real and imagined tool-use pantomimes. *Neurology* **54**, 1331–1336 (2000).
56. M. Mühlau *et al*., Left inferior parietal dominance in gesture imitation: An fMRI study. *Neuropsychologia* **43**, 1086–1098 (2005).
57. K. Y. Haaland, D. L. Harrington, R. T. Knight, Neural representations of skilled movement. *Brain* **123**, 2306–2313 (2000).
58. L. J. Buxbaum, K. Kyle, M. Grossman, H. B. Coslett, Left inferior parietal representations for skilled hand-object interactions: Evidence from stroke and corticobasal degeneration. *Cortex* **43**, 411–423 (2007).
59. R. A. Andersen, H. Cui, Intention, action planning, and decision making in parietal-frontal circuits. *Neuron* **63**, 568–583 (2009).
60. C. J. Stagg *et al*., Polarity and timing-dependent effects of transcranial direct current stimulation in explicit motor learning. *Neuropsychologia* **49**, 800–804 (2011).
61. E. R. Buch *et al*., Effects of tDCS on motor learning and memory formation: A consensus and critical position paper. *Clin. Neurophysiol.* **128**, 589–603 (2017).
62. R. Jalali, R. C. Miall, J. M. Galea, No consistent effect of cerebellar transcranial direct current stimulation on visuomotor adaptation. *J. Neurophysiol.* **118**, 655–665 (2017).
63. J. P. Dmochowski, A. Datta, M. Bikson, Y. Su, L. C. Parra, Optimized multi-electrode stimulation increases focality and intensity at target. *J. Neural. Eng.* **8**, 46011 (2011).
64. D. Edwards *et al*., Physiological and modeling evidence for focal transcranial electrical brain stimulation in humans: A basis for high-definition tDCS. *Neuroimage* **74**, 266–275 (2013).
65. A. T. Sack *et al*., Tracking the mind's image in the brain II: Transcranial magnetic stimulation reveals parietal asymmetry in visuospatial imagery. *Neuron* **35**, 195–204 (2002).
66. N. Dambeck *et al*., Interhemispheric imbalance during visuospatial attention investigated by unilateral and bilateral TMS over human parietal cortices. *Brain Res.* **1072**, 194–199 (2006).
67. S. Cutini, P. Scatturin, M. Zorzi, A new method based on ICBM152 head surface for probe placement in multichannel fNIRS. *Neuroimage* **54**, 919–927 (2011).